High-frequency programmable acoustic wave device realized through ferroelectric domain engineering

Yachin Ivry, Nan Wang, and Colm Durkan

Citation: Applied Physics Letters **104**, 133505 (2014); doi: 10.1063/1.4869823
View online: http://dx.doi.org/10.1063/1.4869823
View Table of Contents: http://scitation.aip.org/content/aip/journal/apl/104/13?ver=pdfcov
Published by the AIP Publishing

High-frequency programmable acoustic wave device realized through ferroelectric domain engineering

Yachin Ivry,[a),b),c)] Nan Wang,[b)] and Colm Durkan[c)]
Nanoscience Centre, University of Cambridge, 11 JJ Thomson Avenue, Cambridge CB3 0FF, United Kingdom

(Received 6 December 2013; accepted 17 March 2014; published online 1 April 2014)

Surface acoustic wave devices are extensively used in contemporary wireless communication devices. We used atomic force microscopy to form periodic macroscopic ferroelectric domains in sol-gel deposited lead zirconate titanate, where each ferroelectric domain is composed of many crystallites, each of which contains many microscopic ferroelastic domains. We examined the electro-acoustic characteristics of the apparatus and found a resonator behavior similar to that of an equivalent surface or bulk acoustic wave device. We show that the operational frequency of the device can be tailored by altering the periodicity of the engineered domains and demonstrate high-frequency filter behavior (>8 GHz), allowing low-cost programmable high-frequency resonators. © *2014 AIP Publishing LLC*. [http://dx.doi.org/10.1063/1.4869823]

Piezoelectrics are functional materials with a strong dependence of strain on applied electric fields. Hence, they have applications ranging from medical ultrasonic imaging to biosensors and actuators[1] and their functionality is essential to some systems in biological entities, e.g., in the growth and repair of bones.[2] Ferroelectrics are a subgroup of piezoelectric materials with the additional functionality of reversible spontaneous polarization. Ferroelectrics are often used due to their relaxor behavior, i.e., the high electromechanical coupling and electrostriction they exhibit. However, generally the additional functionality of reversible polarization is not exploited, except in memory devices.

In conventional RF (radio frequency) piezoelectric-based resonators, an AC voltage is applied between two sets of periodic electrodes that are deposited on the relaxor surface (Fig. 1(a)). The voltage applied across the electrodes is converted into a mechanical strain, σ, due to the inverse piezoelectric effect $\sigma = d^{T}\boldsymbol{E}$, where d^{T} is the inverse piezoelectric matrix and $\boldsymbol{E}$ is the applied electric field. The mechanical energy then propagates via *Rayleigh waves*[3] (mechanical waves that propagate at the surface of a solid, similar to those that propagate after earthquakes) known as Surface Acoustic Waves (SAWs), which in turn are converted back into an AC electric signal when they reach the opposite electrodes, via the direct piezoelectric effect. There is a resonant coupling between the electrodes when their spacing or periodicity is a half-integer multiple of the electro-acoustic wavelength. Since the electro-acoustic wave propagates at the speed of sound of the material, v_s, the fundamental resonance frequency is determined by the electrode periodicity, λ

$$f_0 = v_s/\lambda. \quad (1)$$

The operational frequency of such a device is, therefore, controlled via the configuration of the electrodes, and once fabricated, it is fixed. A key property of Rayleigh waves is that they are highly confined to the surface and decay exponentially into the bulk. Thus, the entire process occurs at the surface of the material, at the electrode-relaxor interface. This means that the signal can propagate without many losses, which is a positive outcome from the technological point of view. However, it imposes severe limitations on the electrode

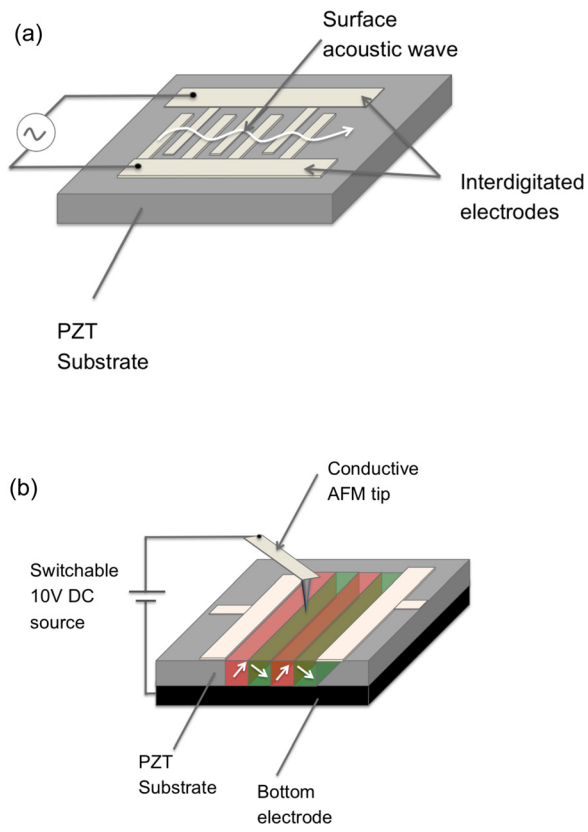

FIG. 1. (a) Schematic of a conventional SAW device. (b) Schematic of the patterning process. 16 domains are engineered using the tip, although we have illustrated 4 here for simplicity. The film is (111) oriented so the polarization will be at 45° to the surface normal.

[a)]Present address: Research Laboratory of Electronics, Massachusetts Institute of Technology, 77 Massachusetts Avenue, Cambridge, Massachusetts 02139, USA.
[b)]Y. Ivry and N. Wang contributed equally to the work.
[c)]Authors to whom correspondence should be addressed. Electronic addresses: ivry@mit.edu and cd229@eng.cam.ac.uk.

periodicity. Practically, the typical periodicity is limited by lithographic processing to around 1 μm. Bearing in mind that for a typical relaxor, v_s is in the range of 2.5–6 km/s, the operational frequency of such SAW devices has a theoretical upper limit of around 6 GHz (purely on the basis of the speed of sound and the spacing of the electrodes), whereas in practice, the SAW filters used in contemporary 3G and 4G cellphone telecommunication networks typically operate below 2.5 GHz. Whilst, in principle, SAW resonators operating at higher frequency (up to 10 GHz) have been demonstrated,[4] with electrodes as small as 90 nm fabricated by electron-beam lithography, the losses associated with the high resistance of such small electrodes rendered the devices somewhat impractical. The electrodes suffer from Joule heating and electromigration[5] and delaminate under high power, which is only overcome by either operating at low temperature (below 10 K) or by using exotic electrode materials. Hence, a device architecture that can operate at high frequency but that can be implemented using larger electrodes could address these issues and is what we report on in this article.

The continuous demand to increase the data transfer rate in wireless systems raises the need for alternative technologies with higher operational frequency and increased bandwidth. Moreover, the enormous increase in wireless devices has created a new demand–*programmable* operational frequency, a feature that cannot exist in conventional SAW devices. To overcome the first limitation of high operational frequencies, bulk acoustic wave (BAW) devices have been developed.[6] These devices typically comprise a thin film of a relaxor sandwiched between two electrodes. However, their complexity and cost have prevented BAW technology from replacing SAW technology in some mainstream devices, although in principle they can outperform SAW devices. BAW filters are now widely used in cell phones.

The concept of using *domains* of different polarization to make a combined SAW-BAW smart resonator was raised by Coldren *et al*. in 1977 (Ref. 7) and was later implemented by Zhu and Minga.[8] Inspired by semiconductor devices that are based on artificially fabricated superlattices that were developed at that time, they designed a structure of periodically alternating ferroelectric domains for a combined SAW-BAW resonator. In this structure, the abrupt difference between the piezoelectric coefficient and dielectric constant of a domain and a domain wall allows the domain walls to act as a δ source of sound waves.[9] Therefore, the resonance frequency is determined by the domain periodicity rather than the periodicity of any electrodes. Zhu and Minga (in a work that was later expanded by Ostrovskiia and Nadtochiy[10]) demonstrated that alternating ferroelectric domains in doped $LiNbO_3$ samples, with $\lambda = 13\,\mu$m resulted in a resonator with $f_0 = 552$ MHz and magnitude loss <30 dB. A rigorous analysis of the electromechanical signal propagation of this case indicated that the signal was carried by *Lamb* waves. However, given that the reported speed of sound of their $LiNbO_3$ sample is $v_s = 7320$ m/s, Eq. (1) predicts the resonance frequency (within an accuracy of ca. 0.5%), an assumption that was also supported by more recent studies.[11]

The reversibility of ferroelectric domains allows one to control their periodicity, hence the increasing importance of the field of domain engineering. Advances in scanning probe microscopy have enabled a convenient method for both controlling and imaging ferroelectric domains in such materials. In particular, piezoresponse force microscopy (PFM)[12–14] allows domain imaging and formation at the scale from a few nanometers to several microns. In this way, periodic ferroelectric domain structures can be created by the scanning PFM tip, as illustrated in Fig. 1(b), and at small-enough scales that can lead to high-frequency devices.

A decade ago, Sarin Kumar *et al*. demonstrated that ferroelectric domains written in a high-quality tetragonal lead zirconate titanate (PZT) film can act as an RF transducer. They used $\lambda = 0.8$–$1.2\,\mu$m and obtained $f_0 = 1.5$–3.5 GHz, with very low losses (<1 dB).[11] PZT is a mainstream relaxor that can be found in many piezoelectric- and ferroelectric-based devices. Therefore, the technological potential of PZT-based programmable high-frequency RF devices is immense. Nevertheless, the operational frequency range they demonstrated is rather similar to that obtained by conventional SAW devices. Furthermore, although high-quality tetragonal PZT films such as those made by Sarin Kumar *et al*. can be made in the lab, for technological applications, lower-cost materials (e.g., sol-gel deposited films) that are usually polycrystalline are preferable. In such materials, not only may the electro-acoustic waves be scattered by the grain boundaries, the existence of twin domains may also scatter such waves, potentially leading to unacceptable losses and undetectable resonances. These factors reduce the attractiveness of periodically alternating domain-engineered devices and may explain why these devices have yet to reach their potential.

We examined the electro-acoustic behavior of a sol-gel deposited 60 nm thick tetragonal PZT film ($Pb_{0.7}Zr_{0.3}TiO_3$), on a Ir bottom electrode on SiO_2 on Si, and with mean grain diameter around 400 nm, similar to those reported elsewhere.[15] The predominant orientation of the film is (111) so the lateral angles between polytwins are multiples of 30°. To implement electro-acoustic scattering measurements, we used electron-beam lithography to fabricate gold electrodes on the PZT surface with three different spacings: 4, 8, and 16 μm. Figure 2(a) shows an optical micrograph of a set of electrodes deposited on the PZT surface. We then used the AFM tip to polarize the area between the electrodes with 16 periodically alternating ferroelectric domain stripes, with period, λ, ranging from 500 nm to 2 μm (the number of periods was chosen to optimize the interplay between a narrower frequency band and the signal losses). Figure 2(b) shows the native domain distribution in the area within two electrodes with 8 μm separation in which periodically poled domains were later written with PFM, while Figs. 2(ba) and 2(bb) show the topography and native domain distribution in three different devices. Given how thin the film is, the polarized domains will extend through the entire thickness of the film, and the acoustic wave that will propagate between the excited electrodes will do so through the film rather than just on the surface.

To evaluate the electrical performance of the resonators, the scattering matrix components were measured via a two-port measurement setup. Electrical measurements were performed using an Agilent N5230C network analyzer in a Suss PM5 III analytical probe station in an ambient environment. For each device, the S_{11} scattering parameter (the return loss) was measured. The significance being of this

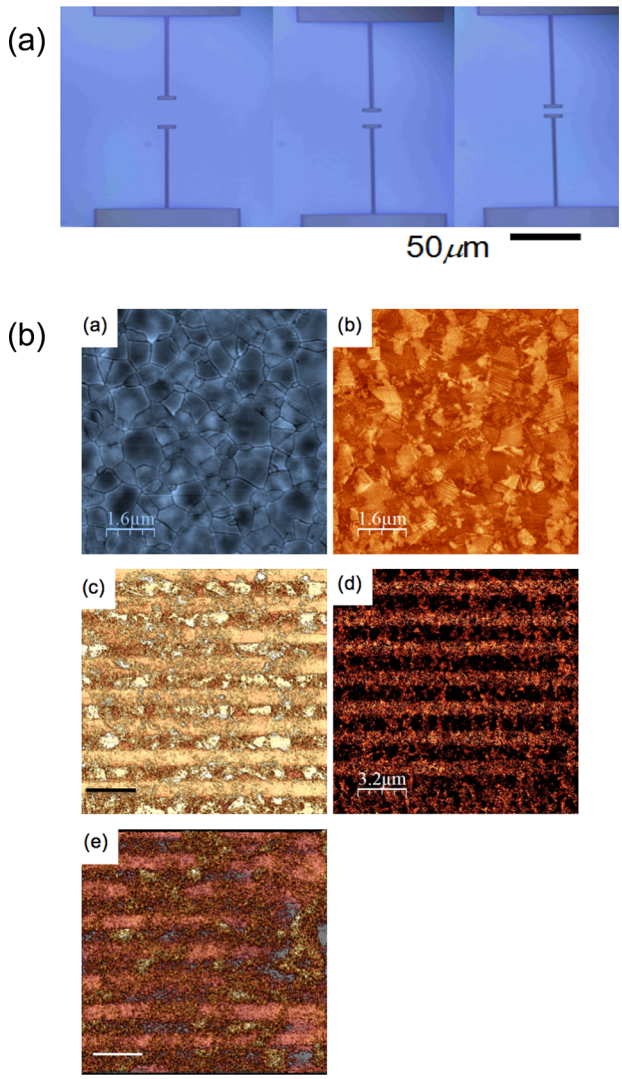

FIG. 2. (a) Optical micrographs of electrodes with 16 μm, 8 μm, and 4 μm gaps, respectively. (b): (a) Topography and polarization distribution in the area between the 8 μm separated electrodes; (b) PFM magnitude imaging before; and (c) PFM phase imaging after domain engineering; (d) and (e) the polarization distributions in the 16 μm and 4 μm devices, respectively, as observed with the PFM phase signals. The scale bars in (c) and (e) are 1.6 μm and 0.8 μm, respectively.

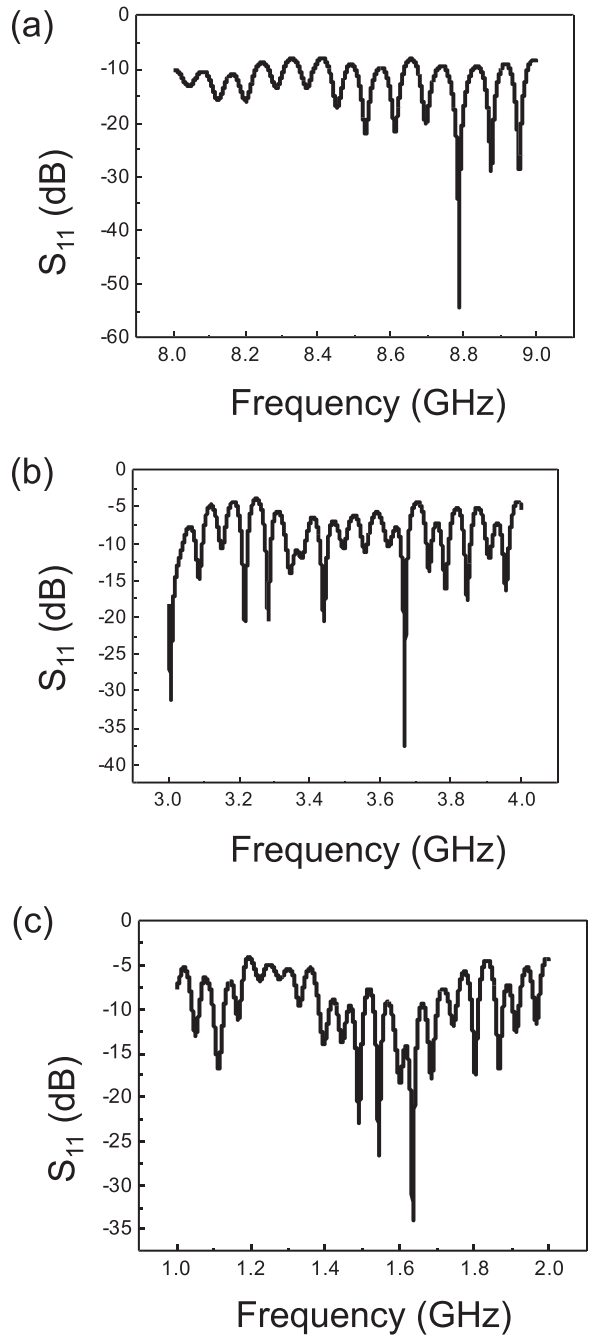

FIG. 3. S_{11} scattering measurements for devices with (a) 16 μm, (b) 8 μm, and (c) 4 μm gap between the metallic electrodes demonstrating a programmable f_0 of (a) 1.63, (b) 3.66, and (c) 8.8 GHz.

measurement scheme is that at the resonant frequency, there will be a significant reduction in S_{11}.

Figure 3 shows the resulting characteristics of the devices where we demonstrate that they each exhibit a reflection minimum (and therefore a transmission maximum) corresponding to a resonance, and the frequency at which this happens is controlled by the domain periodicity, λ, in accordance to Eq. (1). In Fig. 3(a), we show S_{11} measured from a device with 16 μm electrode separation, where $\lambda = 2\,\mu$m. The leading resonance frequency, f_0, was measured to be 1.63 GHz. The expected resonance frequency is in the range of 1.25 to 3 GHz. In Fig. 3(b), we show an 8 μm device where $\lambda = 1\,\mu$m and the resonance frequency is 3.66 GHz, which compares well to the expected range of 2.5 to 6 GHz. In Figure 3(c), we show a 4 μm device where $\lambda = 500$ nm and the resonance frequency is 8.8 GHz, which compares well to the expected range of 5 to 12 GHz. Figure 4(a) presents the linear relation between the dominant resonance frequency and the periodicity of the engineered domains. We can use our data to obtain a better estimate of the speed of sound in our material, and from the best linear fit of $f_0(\lambda)$ to Eq. (1) we find it to be 4.2 ± 0.5 km/s. The level of uncertainty in the speed of sound arises due to the fact that it varies significantly with composition, defect density, and film thickness. In Fig. 4(b), we have plotted the relationship between device size and the reflection loss at resonance. This highlights the fact that the *transmission* losses increase as device size increases.

It was shown by Arlt[16] that a major contribution to dielectric losses comes from ferroelectric and ferroelastic domain wall movement, and that this persists into the GHz range. We would therefore expect that the more domain walls there are between the electrodes, the larger the losses.

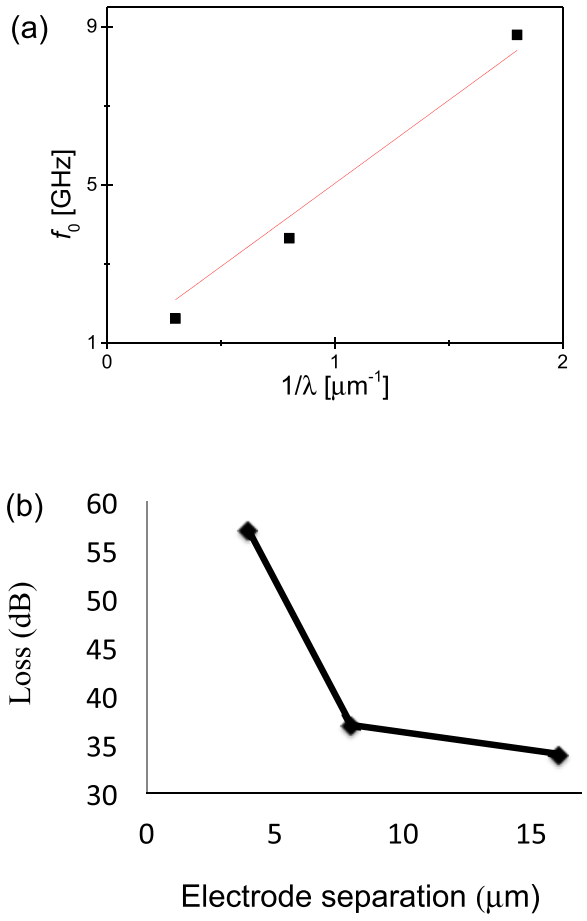

FIG. 4. (a) Linear relationship between the dominant resonant frequency and the inverse periodicity of the engineered domains. The straight line is the linear fit to Eq. (1) suggesting $v_s = 4.2$ km/s (standard errors are 0.25 km/s and $R^2 = 0.975$). (b) Relationship between the reflection loss of the leading resonance and the device size illustrating the decrease in reflection losses (which is interpreted as an increase in transmission losses) with increasing device size.

Given that there are an equal number of ferroelectric domains (16) between each pair of electrodes, then we can conclude that the losses associated with ferroelectric domain wall motion are small compared to other mechanisms, the dominant ones being ferroelastic domain wall motion and scattering from grain boundaries. The domain configurations we encountered in our devices are far more complex than those considered by Arlt, and are not homogeneous, so their model is not straightforward to apply. However, the Debye-like loss characteristics suggest a relaxation frequency in the GHz range for a pure ferroelectric film, and the presence of elastic or electric stress fields will increase this frequency. We therefore suggest that the internal elastic fields associated with the multitude of ferroelastic domain walls within our material serve to greatly increase the relaxation frequency, enough that we are able to observe filter like characteristics up to almost 9 GHz.

Another point to note is that our device configuration only involves one set of two electrodes as opposed to two sets of $>\sim 15$ as is found in a typical SAW device, and ultimately, the domains could be engineered using a conductive contact stamp rather than an AFM tip, so massively parallel fabrication is a possibility, and one could simply re-stamp with different domain periodicity without needing to fabricate an entirely new device.

In summary, we have demonstrated a simple SAW filter configuration where the resonator comprises engineered ferroelectric nano-domains. We have shown that a polycrystalline thin film is capable of transmitting SAW waves beyond 8 GHz.

[1]P. Luginbuhl, N. F. de Rooij, S. D. Collins, G.-A. Racine, N. J. Setter, and K. G. Brooks, Proc. SPIE **2978**, 129 (1997).
[2]A. O. Marino and R. O. Becker, Nature **228**, 473 (1970).
[3]J. W. S. Rayleigh, Proc. London Math. Soc. **17**, 4 (1885).
[4]K. Yamanouchi, Hideyuki Nakagawa, J. A. Qureshi, and H. Odagawa, Jpn. J. Appl. Phys., Part 1 **38**, 3270 (1999).
[5]F. Hadeed and C. Durkan, Appl. Phys. Lett. **91**, 123120 (2007).
[6]Y. Satoh, T. Nishihara, T. Yokoyama, M. Ueda, and T. Miyashita, Jpn. J. Appl. Phys., Part 1 **44**, 2883 (2005).
[7]B. A. Coldren, A. M. Glass, and R. A. Lemons, "Acoustic wave device," U.S. patent 4,117,424 (30 March 1977).
[8]Y.-Y. Zhu and N.-B. Minga, J. Appl. Phys. **72**, 904 (1992).
[9]H. E. Bömmel and K. Dransfeld, Phys. Rev. **117**, 1245 (1960).
[10]I. V. Ostrovskiia and A. B. Nadtochiy, Appl. Phys. Lett. **86**, 222902 (2005).
[11]A. K. Sarin Kumar, P. Paruch, J.-M. Triscone, W. Daniau, S. Ballandras, L. Pellegrino, D. Marré, and T. Tybell, Appl. Phys. Lett. **85**, 1757 (2004).
[12]P. Guthner and K. Dransfeld, Appl. Phys. Lett. **61**, 1137 (1992).
[13]S. V. Kalinin and D. A. Bonnell, Phys. Rev. B **65**, 125408 (2002).
[14]C. Durkan, D. P. Chu, P. Migliorato, and M. E. Welland, Appl. Phys. Lett. **76**, 366 (2000).
[15]Y. Ivry, D. P. Chu, and C. Durkan, Appl. Phys. Lett. **94**, 162903 (2009).
[16]G. Arlt, U. Böttinger, and S. Witte, Ann. Phys. **506**, 578 (1994).